



Oral Presentation



HASPER: An Image Repository for Hand Shadow Puppet Recognition

Presented by
Syed Rifat Raiyan

Co-authors

Zibran Zarif Amio, Sabbir Ahmed
Department of Computer Science and Engineering
Islamic University of Technology



Workshop on Cultural Continuity of Artists

Introduction

What is Hand Shadow Puppetry?

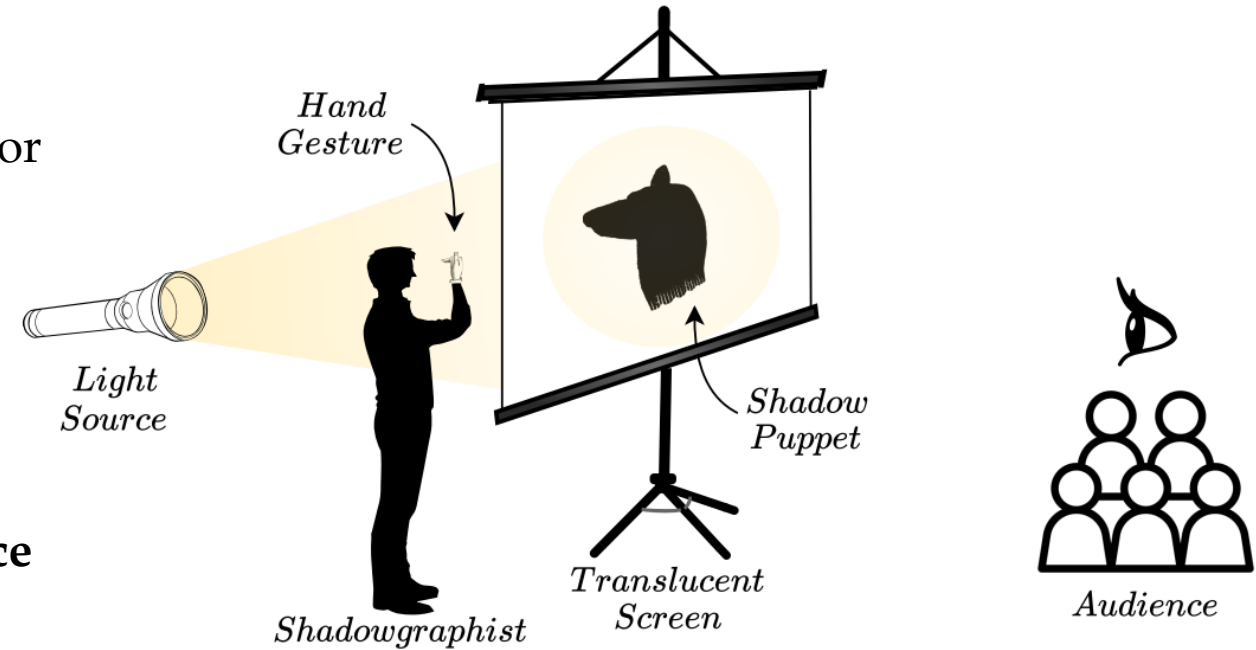
Definition:

Hand Shadow Puppetry, also known as *shadowgraphy* or *ombromanie* is the art of performing a story or show using images made through the construction and manipulation of shadow figures or silhouettes, using one's hands, body, or props [1].

How does it work?

The puppeteer places his **hands between a light source and a translucent screen** to create shadows or silhouettes that resemble different **animals**.

- Also known as *cinema in silhouette*
- On the verge of extinction—UNESCO designated shadow puppetry an **endangered** Intangible Cultural Heritage [2] in 2011 (hence, needs **preservation!**)



(a) A generic hand shadow puppetry setup.



(b) Rabbit



(c) Bird



(d) Dog

Fig: Ombromanie in a nutshell.

Motivation

Our Inspiration to Pursue this Topic

- **Novelty factor:** To the best of our knowledge, **no** explicitly vision-related work or dataset exists on this topic of hand shadow puppet classification.
 - Some of the closely related works will be mentioned in a bit...
- **Gap:** Frontier image generator models are **very bad** at ombromanie.
- **Utility:**
 - ✓ **Tool for teaching** performance art
 - ✓ **Recreational app** for kids
 - ✓ Enabling the development of sophisticated algorithms for automatic **recognition, classification**, or even **generation** of ombromanie performances
- **Nostalgia** — incentivized by childhood memories during the load-shedding days.



ByteDance Seedream-4



xAI Grok 4



Google Imagen-4 Fast



Stable Diffusion 3.5



Google Gemini 2.5 Pro



Tencent Hunyuan 3

Related Work and Dataset

Research Literature on Shadow Puppetry

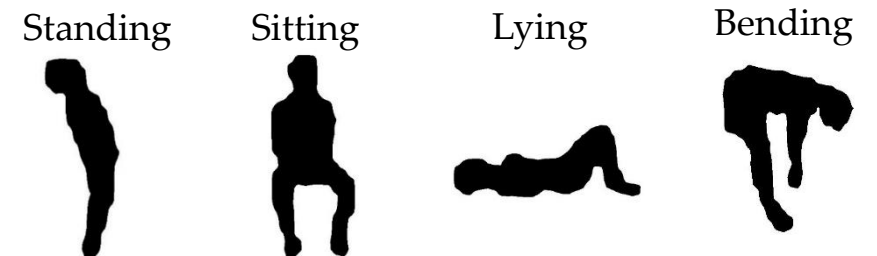
As mentioned before, we **haven't found any prominent work** on hand shadow puppet image classification.

Prominent Works: (**closely related** topics)

- In **Robotics**,
 - (Huang *et al.*)[3] — introduced a framework that enables **robotic arms** to **perform hand shadow puppetry** by matching shape correspondences of input image.
- In **Human-Computer Interaction**,
 - (Zhang *et al.*)[4] — worked on **emulating** the movements and body **gestures of a performer** on **Chinese shadow puppets** using Kinect sensor.
 - (Carr *et al.*)[5] — built a real-time **Indonesian shadow puppet** storytelling application using the Microsoft Kinect sensor capable of **mimicking full-body actions** of user.
- In **Computer Graphics**,
 - (Huang *et al.*)[6] — generated **3D models** of animals from shadow puppet images.

Dataset:

- Human Posture Silhouettes [7] — 4,800 binary images of silhouettes used for **human posture recognition**.

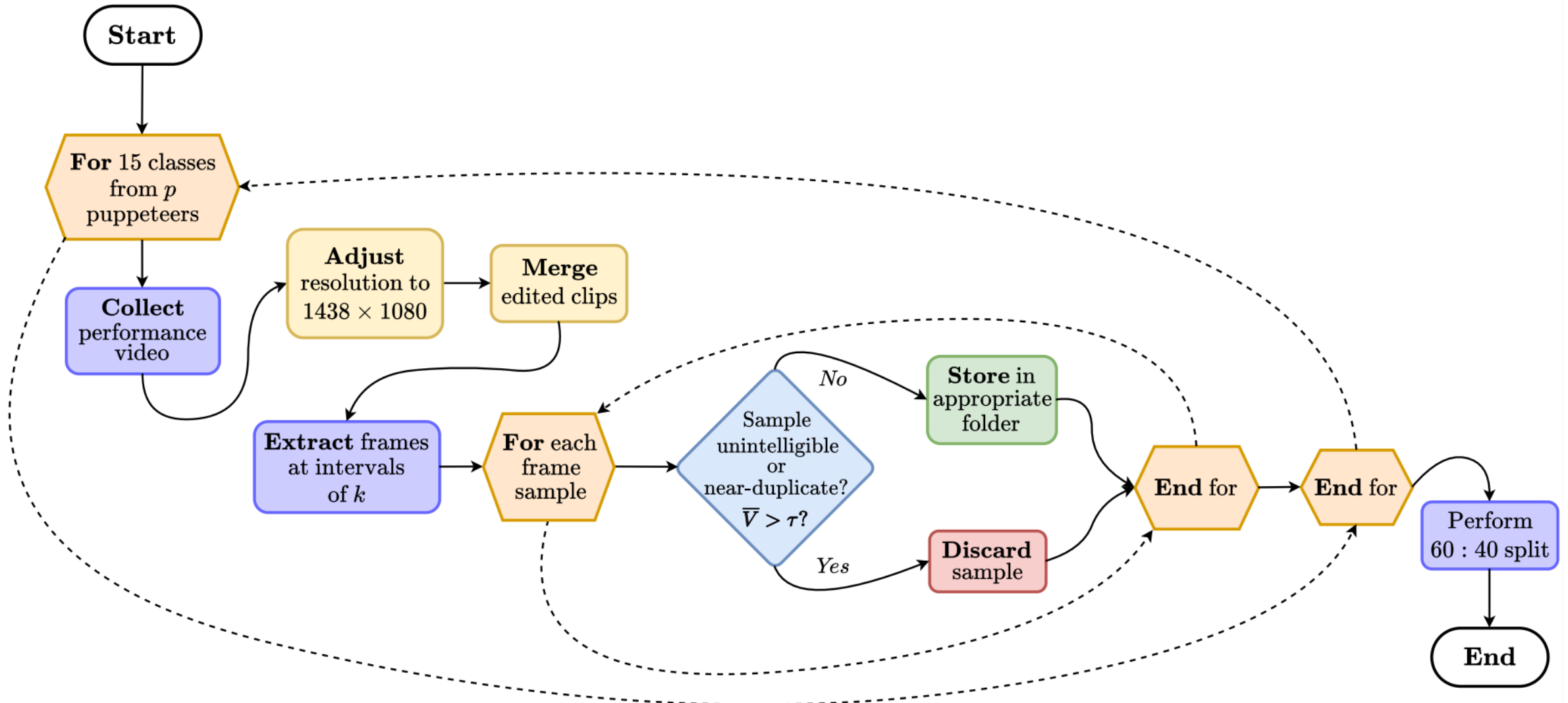


Our Work

What the project entails

- **Data Collection** — Gathered a total of **15,000 images** of hand shadow puppets.
 - ✓ From **68 professional** hand shadow puppeteer clips and **90 amateur** clips.
 - ✓ Across **15** classes.
- **Benchmarking** — Established benchmarks for the dataset.
 - ✓ With **31** SoTA pre-trained Pytorch feature extractor architectures as baselines.
 - ✓ Found superiority of **skip-connected convolutional models** over **attention-based transformers models** in silhouette classification.
 - ✓ Experimented with feature fusion techniques
 - Topological features
 - Silhouette polygonization
- **Prototype Application** — Developed a lightweight Android app using Flutter for real-time classification of hand shadow puppets from camera feeds

Dataset Construction Flowchart



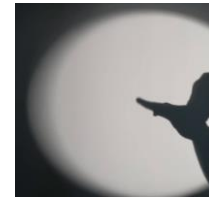
HASPER

Collating Clips

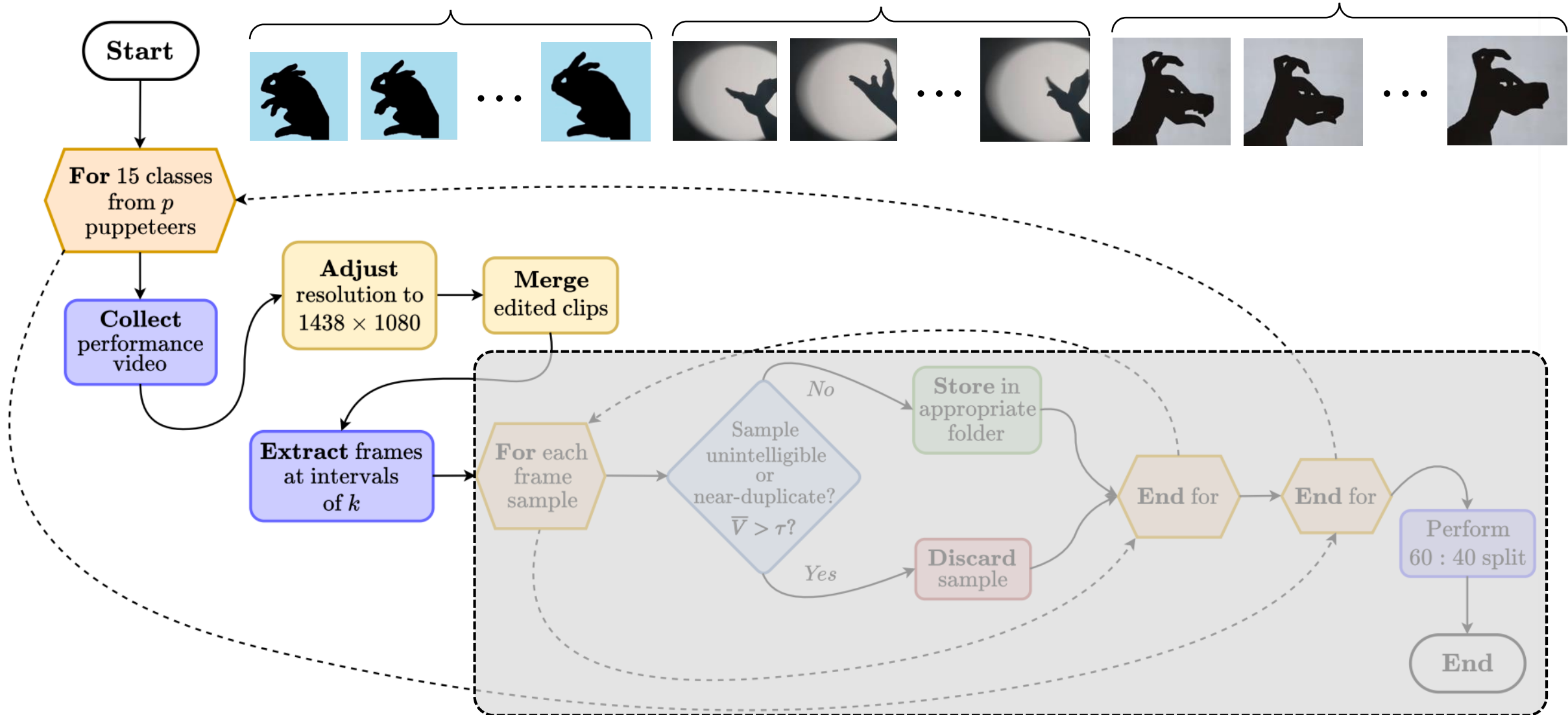
Rabbit

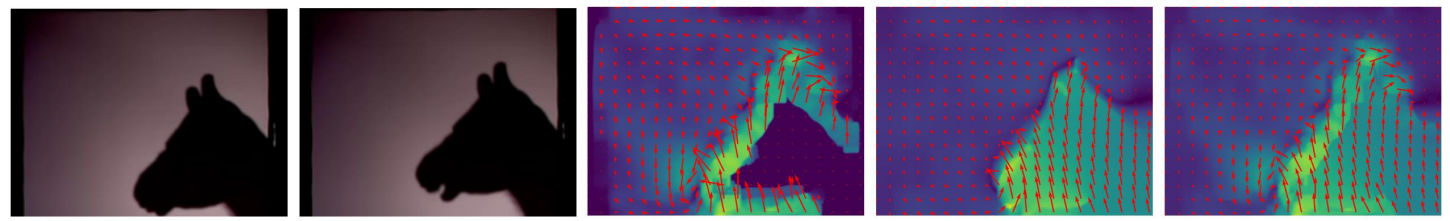


Bird



Dog





(a) t th frame

(b) $(t+k)$ th frame

(c) LK method

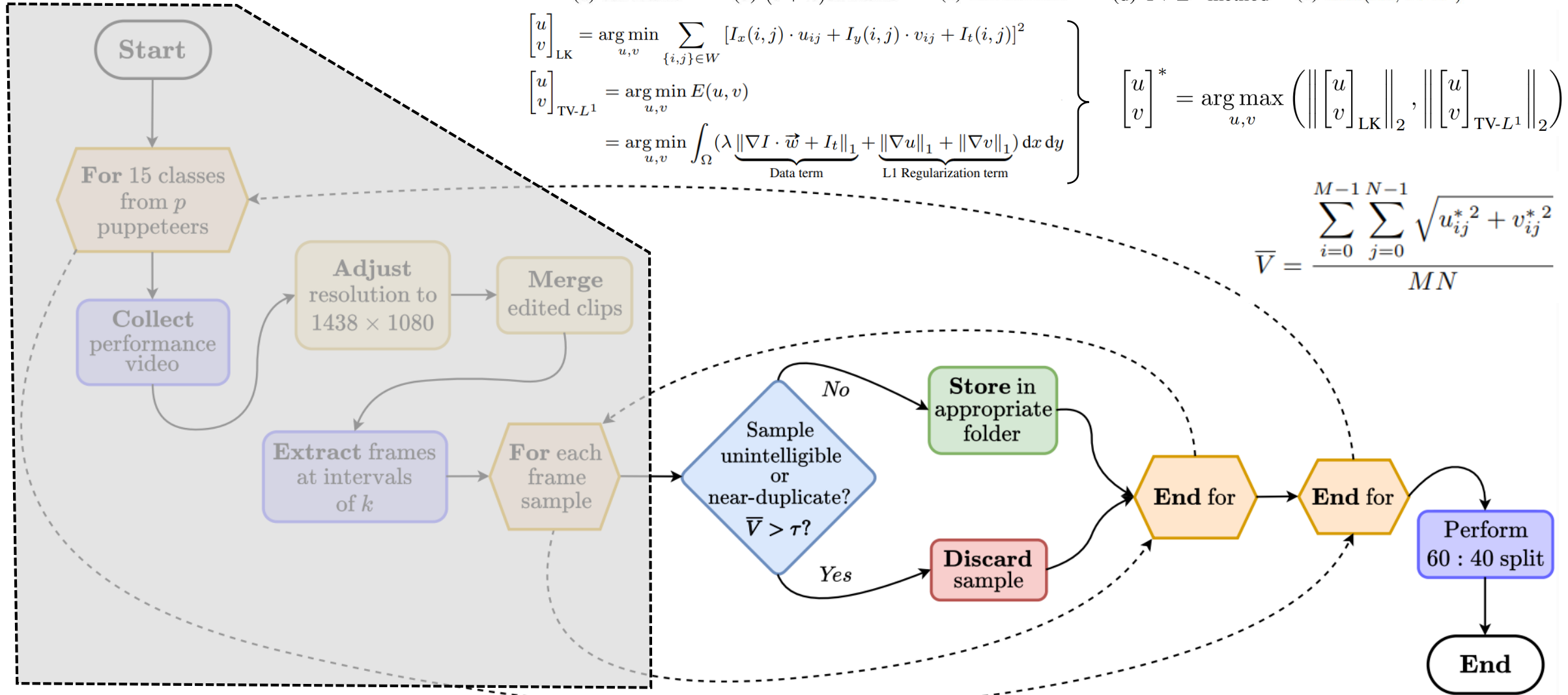
(d) $TV-L^1$ method

(e) $\max(LK, TV-L^1)$

$$\begin{aligned} \begin{bmatrix} u \\ v \end{bmatrix}_{LK} &= \arg \min_{u,v} \sum_{\{i,j\} \in W} [I_x(i,j) \cdot u_{ij} + I_y(i,j) \cdot v_{ij} + I_t(i,j)]^2 \\ \begin{bmatrix} u \\ v \end{bmatrix}_{TV-L^1} &= \arg \min_{u,v} E(u,v) \\ &= \arg \min_{u,v} \int_{\Omega} \underbrace{(\lambda \|\nabla I \cdot \vec{w} + I_t\|_1)}_{\text{Data term}} + \underbrace{(\|\nabla u\|_1 + \|\nabla v\|_1)}_{\text{L1 Regularization term}} dx dy \end{aligned}$$

$$\begin{bmatrix} u \\ v \end{bmatrix}^* = \arg \max_{u,v} \left(\left\| \begin{bmatrix} u \\ v \end{bmatrix}_{LK} \right\|_2, \left\| \begin{bmatrix} u \\ v \end{bmatrix}_{TV-L^1} \right\|_2 \right)$$

$$\bar{V} = \frac{\sum_{i=0}^{M-1} \sum_{j=0}^{N-1} \sqrt{u_{ij}^{*2} + v_{ij}^{*2}}}{MN}$$



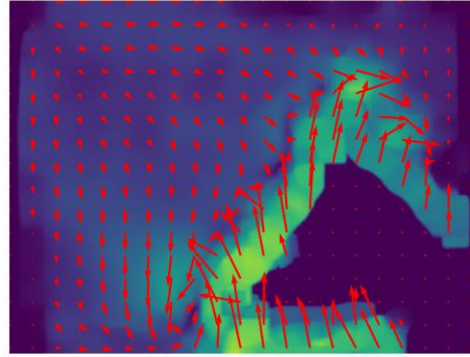
Optical Flow Estimation



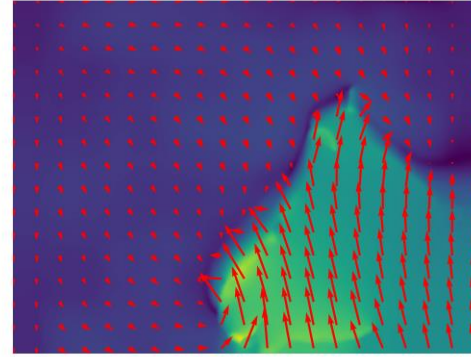
(a) t th frame



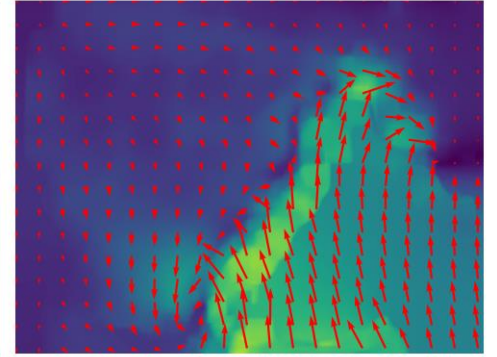
(b) $(t + k)$ th frame



(c) LK method [8]



(d) TV- L^1 method [9]



(e) $\max(\text{LK}, \text{TV-}L^1)$

$$\left. \begin{aligned} \begin{bmatrix} u \\ v \end{bmatrix}_{\text{LK}} &= \arg \min_{u,v} \sum_{\{i,j\} \in W} [I_x(i,j) \cdot u_{ij} + I_y(i,j) \cdot v_{ij} + I_t(i,j)]^2 \\ \begin{bmatrix} u \\ v \end{bmatrix}_{\text{TV-}L^1} &= \arg \min_{u,v} E(u,v) \\ &= \arg \min_{u,v} \int_{\Omega} \underbrace{(\lambda \|\nabla I \cdot \vec{w} + I_t\|_1)}_{\text{Data term}} + \underbrace{(\|\nabla u\|_1 + \|\nabla v\|_1)}_{\text{L1 Regularization term}} dx dy \end{aligned} \right\} \begin{bmatrix} u \\ v \end{bmatrix}^* = \arg \max_{u,v} \left(\left\| \begin{bmatrix} u \\ v \end{bmatrix}_{\text{LK}} \right\|_2, \left\| \begin{bmatrix} u \\ v \end{bmatrix}_{\text{TV-}L^1} \right\|_2 \right)$$

$$\bar{V} = \frac{\sum_{i=0}^{M-1} \sum_{j=0}^{N-1} \sqrt{u_{ij}^{*2} + v_{ij}^{*2}}}{MN}$$

Dataset Statistics

Silhouette Class	Clips		Sample Distribution		
	Pro.	Nov.	Training	Validation	Total
Bird	6	6	600	400	1000
Chicken	2	6	600	400	1000
Cow	2	6	600	400	1000
Crab	4	6	600	400	1000
Deer	6	6	600	400	1000
Dog	7	6	600	400	1000
Elephant	5	6	600	400	1000
Horse	8	6	600	400	1000
Llama	2	6	600	400	1000
Moose	3	6	600	400	1000
Panther	2	6	600	400	1000
Rabbit	4	6	600	400	1000
Snail	4	6	600	400	1000
Snake	3	6	600	400	1000
Swan	10	6	600	400	1000
Total	68	90	9000	6000	15000
	158				

Fig: Statistical summary of HASPER.

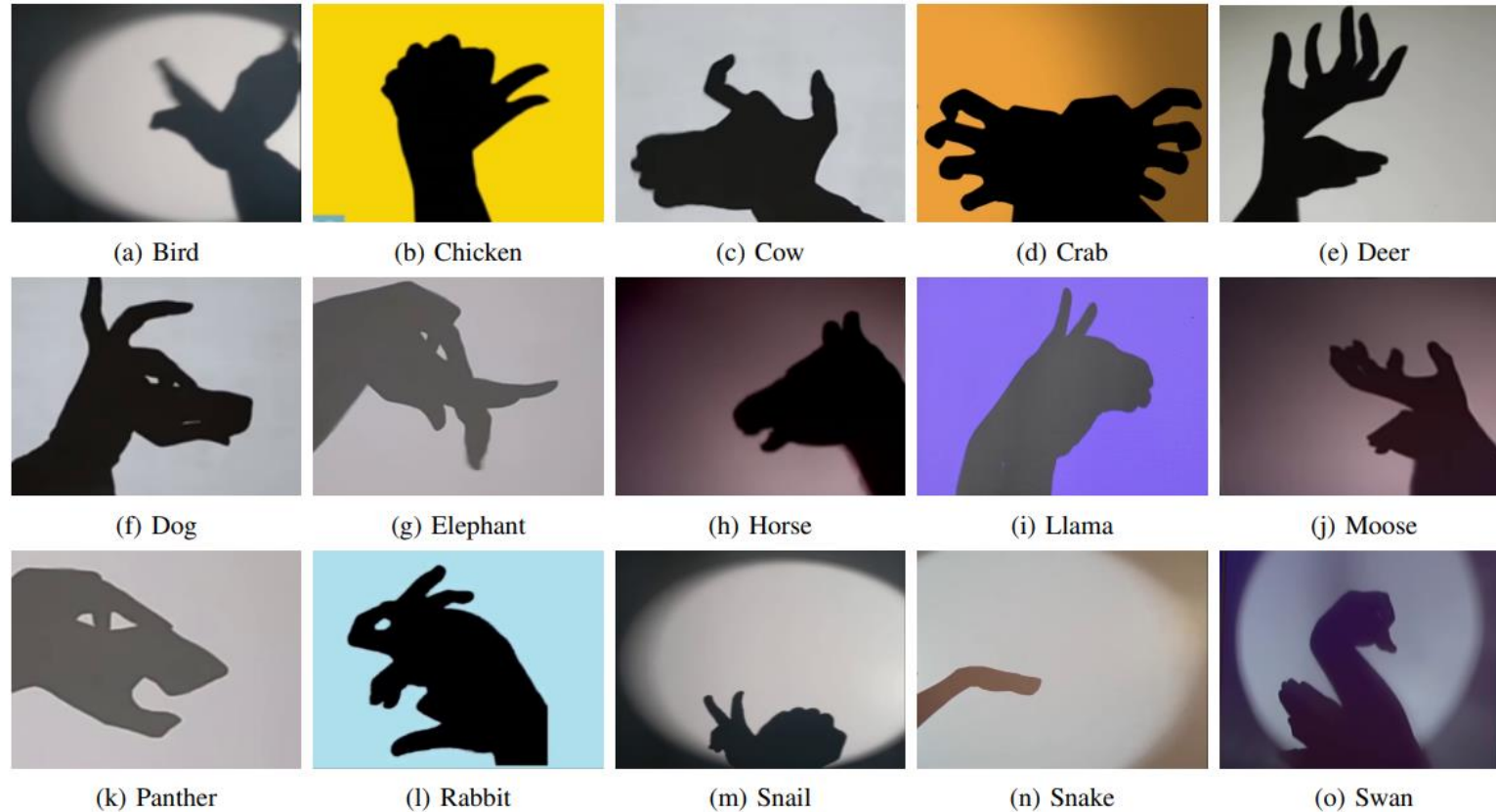


Fig: Samples from each class of the dataset.

- For each class, **professional** $\approx 47.827 \pm 1.414\%$ and **amateur** $\approx 52.172 \pm 1.414\%$
- Proportions of professionally sourced samples belonging to the 'Llama' and 'Snake' classes (14% and 27.3% respectively) are slightly low due to a **scarcity** of performance clips.

Sample Diversity

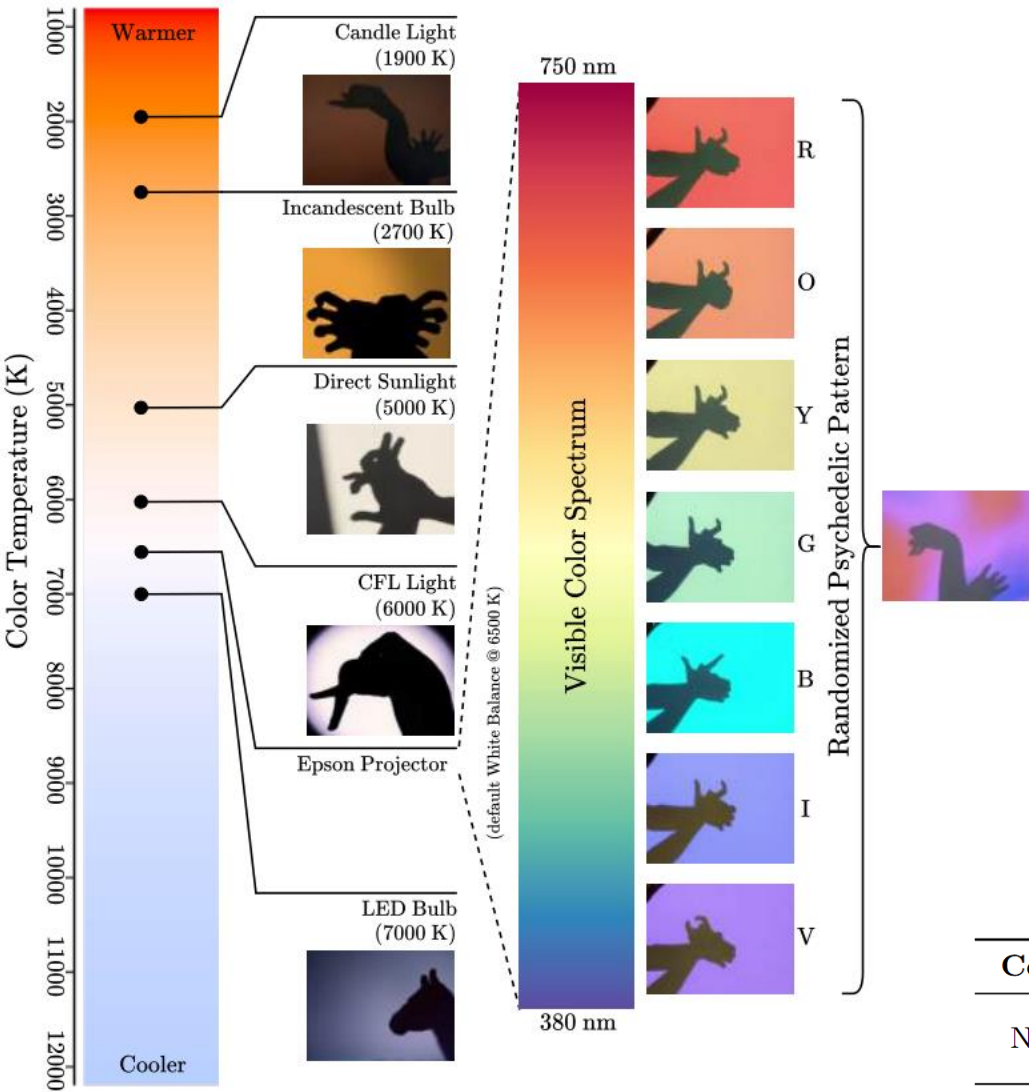
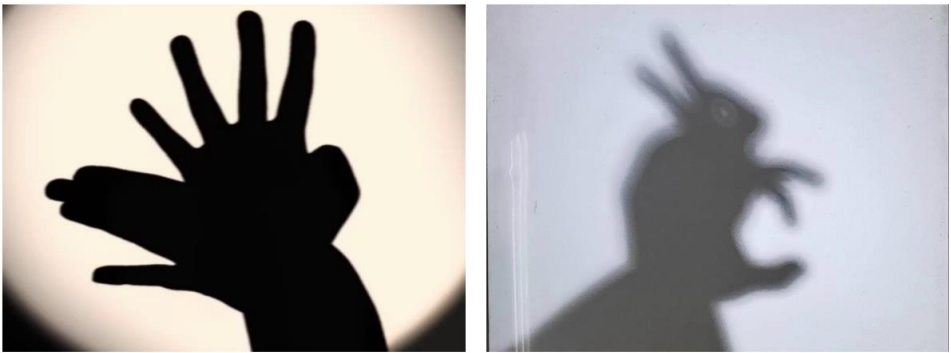


Fig: Light sources for background diversity.



(a) Sharp, high opacity (b) Diffuse, low opacity

Fig: Samples with different silhouette properties.



Fig: ‘Deer’ samples with different artistic representations.

Cohort	Subgroup	<i>n</i>	Gender (M:F)	Age Range	Hand Length (cm)	Hand Width (cm)
Novice	Adults	6	3:3	9 to 25	18.75 ± 1.55	8.66 ± 0.77
	Minors				14.23 ± 1.16	6.73 ± 0.82
Professional	–	14	12:2	N/A	N/A	N/A

Benchmarking

Models and Modifications

- **Feature Extractor Models** — 31 SoTA baselines pre-trained on ImageNet
 - ✓ With a vanilla fully-connected layer
 - ✓ With a simple adapter block
 - ✓ With feature fusions (*concat*)
- **Silhouette Polygonization [10]**
 - Vertex coordinates
- **Topological Features [11]**
 - Betti curves
 - Morphological features
 - Local extrema coordinates
 - Euler characteristic
 - Gradient magnitude
 - Contours

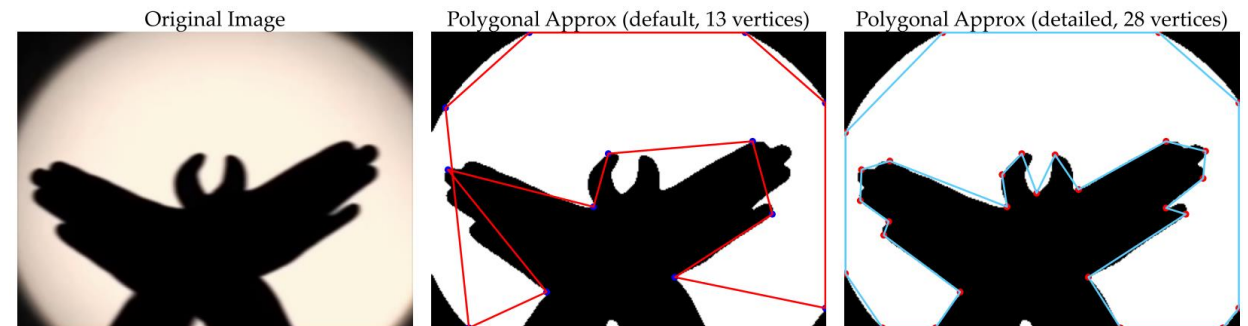
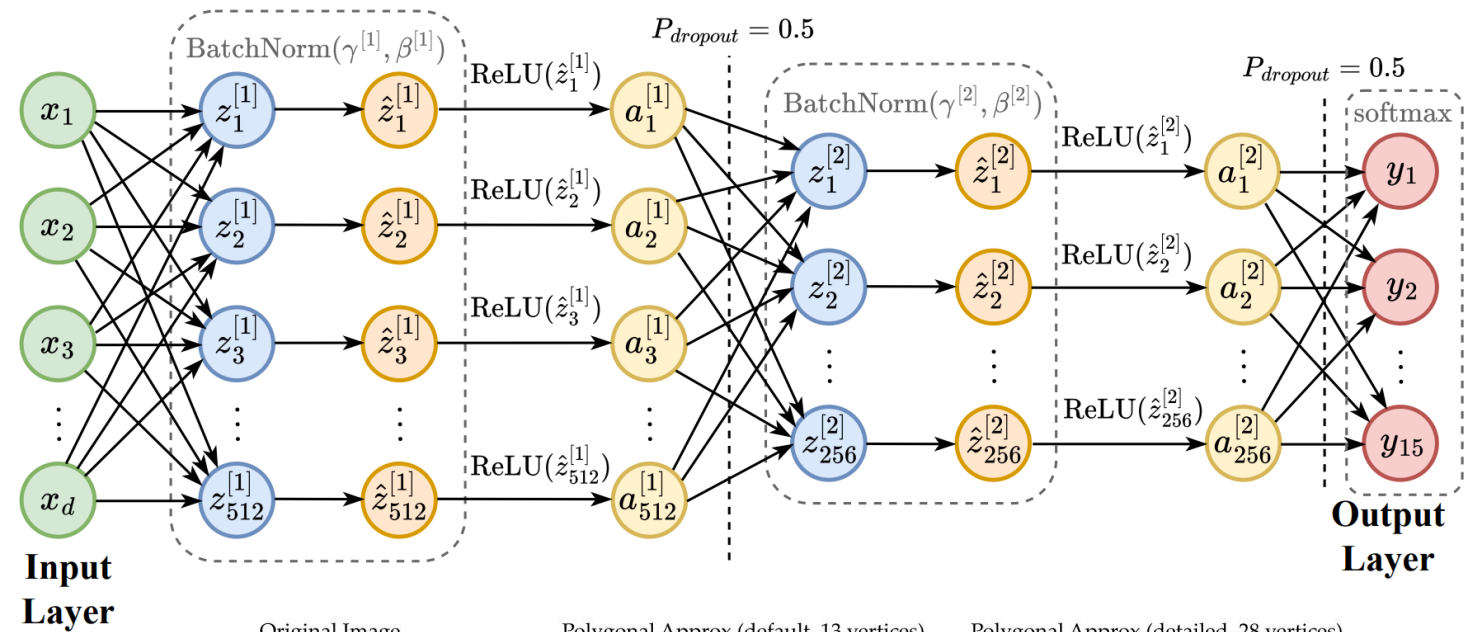


Fig: Polygonal approximations for a hand shadow puppet silhouette.

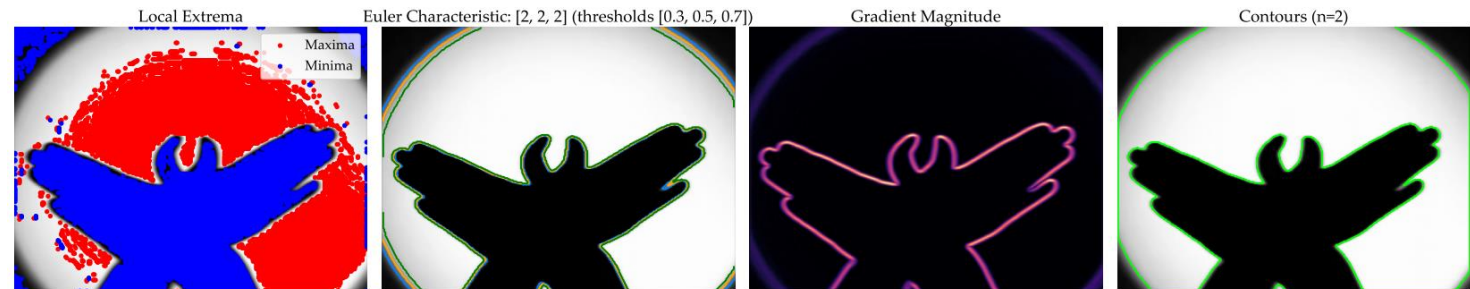


Fig: Topological features for a hand shadow puppet silhouette.

Results

Tentative Benchmarking Results

Metrics:

- Top-*k* accuracy
- Precision
- Recall
- F1-score

Hyperparameters:

- $\alpha = 0.001$
- $\gamma_{momentum} = 0.9$
- $\gamma_{decay} = 0.1$ per 5
- Epochs = 50

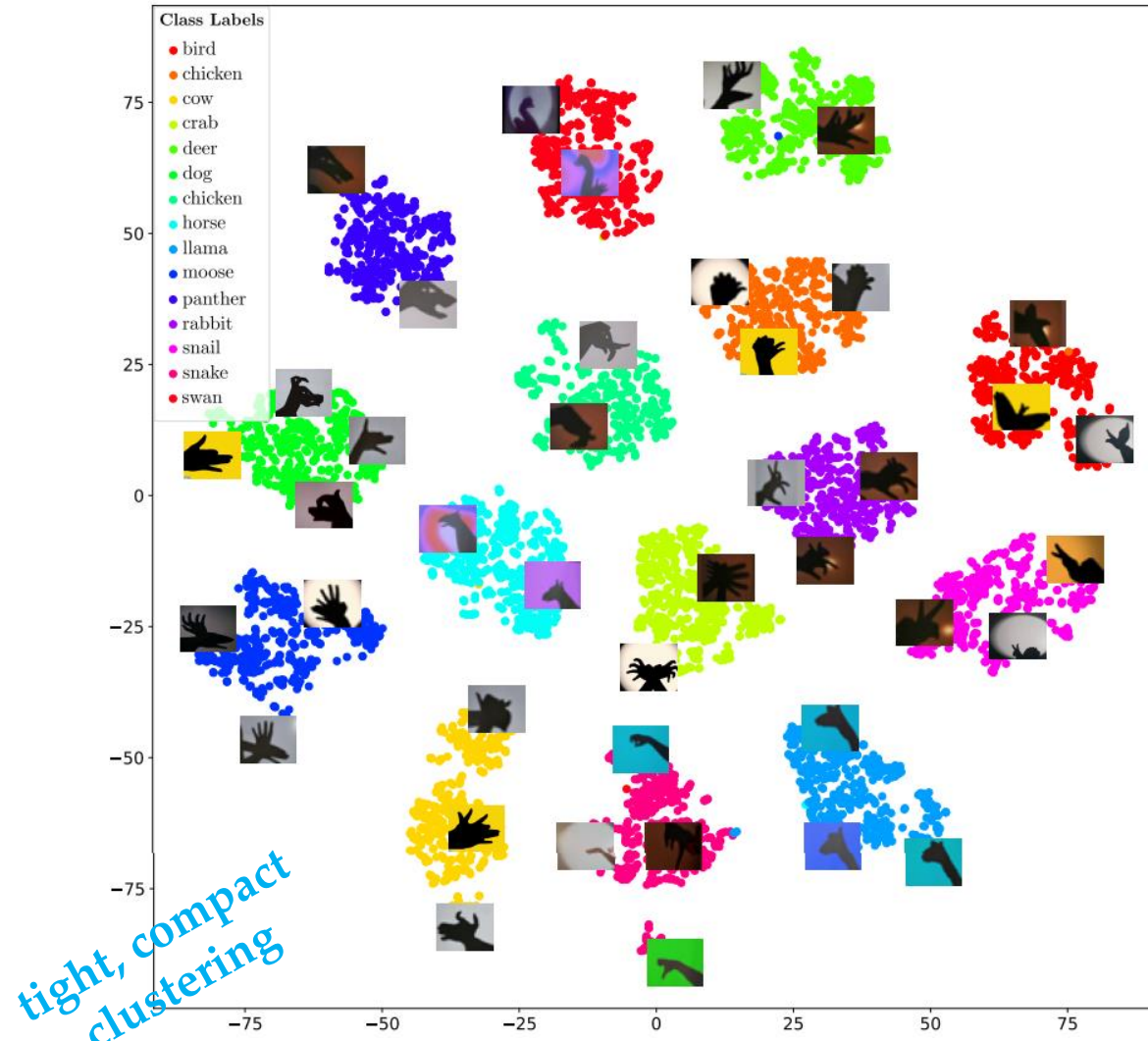
Models	Params.	Performance Metrics											
		Vanilla						w/ Classifier Block					
		Top- <i>k</i> Accuracy (%)			Precision	Recall	F1-score	Top- <i>k</i> Accuracy (%)			Precision	Recall	F1-score
		Top-1	Top-2	Top-3				Top-1	Top-2	Top-3			
SHUFFLENETV2X10 [40]	2.3M	61.73	78.41	86.10	0.6559	0.6173	0.5970	88.73	93.98	96.10	0.8995	0.8873	0.8853
ViTB16 [41]	86.6M	69.71	77.60	83.28	0.7276	0.6972	0.6969	68.88	76.65	81.36	0.7192	0.6868	0.6851
ViTL32 [41]	306.5M	85.10	91.56	94.48	0.8720	0.8510	0.8509	84.71	91.80	94.08	0.8632	0.8472	0.8465
ALEXNET [11]	61.1M	87.01	93.61	95.46	0.8840	0.8702	0.8708	88.18	92.58	94.80	0.8887	0.8818	0.8809
SQUEEZENET1_1 [42]	1.2M	87.56	92.45	94.15	0.8880	0.8757	0.8744	86.21	92.48	94.65	0.8754	0.8622	0.8637
MOBILENETV3SMALL [43]	2.5M	89.48	94.31	95.76	0.9038	0.8948	0.8942	89.85	94.35	96.48	0.9082	0.8985	0.8976
SWINB [44]	87.8M	90.50	95.38	97.40	0.9128	0.9050	0.9042	90.20	95.40	97.08	0.9097	0.902	0.9006
GOOGLENET [45]	6.6M	90.73	94.65	95.70	0.9105	0.9073	0.9059	92.18	95.65	96.58	0.9283	0.9218	0.9206
RESNET18 [46]	11.7M	90.91	95.28	96.60	0.9176	0.9092	0.9069	91.25	95.43	97.05	0.9229	0.9125	0.9119
MOBILENETV3LARGE [43]	5.5M	91.20	94.48	95.98	0.9185	0.9120	0.9110	90.40	94.53	95.26	0.9147	0.9040	0.9024
CONVNEXT [47]	88.6M	91.46	96.33	98.05	0.9220	0.9147	0.9140	92.55	96.36	97.96	0.9306	0.9255	0.9246
SWINV2B [48]	87.9M	91.58	96.25	97.61	0.9210	0.9158	0.9151	91.48	96.00	97.55	0.9209	0.9148	0.9144
VGG16 [12]	138.4M	91.61	95.08	96.65	0.9248	0.9162	0.9168	91.00	95.21	96.45	0.9235	0.9100	0.9119
MNASNET13 [49]	6.3M	91.66	95.65	97.01	0.9240	0.9167	0.9149	91.45	95.86	97.26	0.9231	0.9145	0.9133
CONVNEXTLARGE [47]	197.8M	91.88	95.90	97.70	0.9254	0.9188	0.9181	88.00	94.70	96.56	0.8942	0.8800	0.8782
EFFICIENTNETB0 [50]	5.3M	91.93	95.26	96.71	0.9257	0.9193	0.9178	90.40	93.75	95.10	0.9131	0.9040	0.9022
MAXViT [51]	30.9M	92.01	96.50	97.81	0.9268	0.9202	0.9214	92.08	95.98	97.36	0.9320	0.9208	0.9237
EFFICIENTNETV2S [52]	21.5M	92.31	95.75	96.76	0.9375	0.9232	0.9245	94.45	97.35	98.30	0.9498	0.9445	0.9438
VGG19 [12]	143.7M	92.36	95.13	96.10	0.9354	0.9237	0.9242	91.80	95.06	96.15	0.9296	0.9180	0.9187
MOBILENETV2 [53]	3.5M	92.38	94.98	96.05	0.9303	0.9238	0.9233	92.31	95.38	96.91	0.9311	0.9232	0.9225
WIDERESNET50_2 [54]	68.9M	92.46	96.28	97.28	0.9331	0.9247	0.9235	93.35	95.73	97.15	0.9421	0.9335	0.9330
RESNET50 [46]	25.6M	92.58	95.56	96.75	0.9332	0.9258	0.9252	93.08	96.48	97.20	0.9363	0.9308	0.9299
REGNETX32GF [55]	107.8M	92.86	95.71	96.93	0.9348	0.9287	0.9269	92.91	95.71	96.95	0.9366	0.9292	0.9282
DENSENET121 [56]	8.0M	92.93	95.75	96.88	0.9367	0.9293	0.9282	92.95	95.51	96.56	0.9360	0.9295	0.9285
RESNEXT101_32X8D [57]	88.8M	93.00	96.41	97.23	0.9364	0.9310	0.9303	94.20	96.61	97.58	0.9520	0.9420	0.9423
WIDERESNET101_2 [54]	126.9M	93.36	95.81	96.90	0.9423	0.9337	0.9332	92.73	96.35	97.63	0.9337	0.9273	0.9267
INCEPTIONV3 [58]	27.2M	93.50	96.48	97.35	0.9401	0.9350	0.9338	93.71	96.36	97.06	0.9446	0.9372	0.9371
DENSENET201 [56]	20.0M	93.56	95.78	96.73	0.9450	0.9357	0.9353	94.43	97.00	97.61	0.9492	0.9443	0.9442
RESNET101 [46]	44.5M	93.81	96.23	97.71	0.9432	0.9382	0.9406	93.23	96.93	98.13	0.9386	0.9323	0.9321
RESNET152 [46]	60.2M	94.06	97.06	98.05	0.9447	0.9407	0.9394	93.05	96.73	97.48	0.9374	0.9305	0.9297
RESNET34 [46]	21.8M	94.97	97.23	98.23	0.9516	0.9497	0.9491	91.98	95.95	97.20	0.9266	0.9198	0.9189
RESNET34 w/ Silhouette Polygonization	21.8M	92.72	96.41	97.51	0.9328	0.9272	0.9257	92.95 (+1.05%)	95.75	96.61	0.9352 (+0.93%)	0.9295 (+1.05%)	0.9283 (+1.02%)
RESNET34 w/ Topological Features	21.8M	93.72	96.43	97.78	0.9432	0.9372	0.9359	94.05 (+2.25%)	96.45 (+0.52%)	97.53 (+0.34%)	0.9476 (+2.27%)	0.9405 (+2.25%)	0.9401 (+2.31%)

Models	Params.	Performance Metrics											
		Vanilla						w/ Classifier Block					
		Top- <i>k</i> Accuracy (%)			Precision	Recall	F1-score	Top- <i>k</i> Accuracy (%)			Precision	Recall	F1-score
		Top-1	Top-2	Top-3				Top-1	Top-2	Top-3			
SHUFFLENETV2X10 [40]	2.3M	61.73	78.41	86.10	0.6559	0.6173	0.5970	88.73	93.98	96.10	0.8995	0.8873	0.8853
ViTB16 [41]	86.6M	69.71	77.60	83.28	0.7276	0.6972	0.6969	68.88	76.65	81.36	0.7192	0.6868	0.6851
ViTL32 [41]	306.5M	85.10	91.56	94.48	0.8720	0.8510	0.8509	84.71	91.80	94.08	0.8632	0.8472	0.8465
ALEXNET [11]	61.1M	87.01	93.61	95.46	0.8840	0.8702	0.8708	88.18	92.58	94.80	0.8887	0.8818	0.8809
SQUEEZE1_1 [42]	1.2M	87.56	92.45	94.15	0.8880	0.8757	0.8744	86.21	92.48	94.65	0.8754	0.8622	0.8637
MOBILENETV3SMALL [43]	2.5M	89.48	94.31	95.76	0.9038	0.8948	0.8942	89.85	94.35	96.48	0.9082	0.8985	0.8976
SWINB [44]	87.8M	90.50	95.38	97.40	0.9128	0.9050	0.9042	90.20	95.40	97.08	0.9097	0.902	0.9006
GOOGLENET [45]	6.6M	90.73	94.65	95.70	0.9105	0.9073	0.9059	92.18	95.65	96.58	0.9283	0.9218	0.9206
RESNET18 [46]	11.7M	90.91	95.28	96.60	0.9176	0.9092	0.9069	91.25	95.43	97.05	0.9229	0.9125	0.9119
MOBILENETV3LARGE [43]	5.5M	91.20	94.48	95.98	0.9185	0.9120	0.9110	90.40	94.53	95.26	0.9147	0.9040	0.9024
CONVNEXT [47]	88.6M	91.46	96.33	98.05	0.9220	0.9147	0.9140	92.55	96.36	97.96	0.9306	0.9255	0.9246
SWINV2B [48]	87.9M	91.58	96.25	97.61	0.9210	0.9158	0.9151	91.48	96.00	97.55	0.9209	0.9148	0.9144
VGG16 [12]	138.4M	91.61	95.08	96.65	0.9248	0.9162	0.9168	91.00	95.21	96.45	0.9235	0.9100	0.9119
MNASNET13 [49]	6.3M	91.66	95.65	97.01	0.9240	0.9167	0.9149	91.45	95.86	97.26	0.9231	0.9145	0.9133
CONVNEXTLARGE [47]	197.8M	91.88	95.90	97.70	0.9254	0.9188	0.9181	88.00	94.70	96.56	0.8942	0.8800	0.8782
EFFICIENTNETB0 [50]	5.3M	91.93	95.26	96.71	0.9257	0.9193	0.9178	90.40	93.75	95.10	0.9131	0.9040	0.9022
MAXViT [51]	30.9M	92.01	96.50	97.81	0.9268	0.9202	0.9214	92.08	95.98	97.36	0.9320	0.9208	0.9237
EFFICIENTNETV2S [52]	21.5M	92.31	95.75	96.76	0.9375	0.9232	0.9245	94.45	97.35	98.30	0.9498	0.9445	0.9438
VGG19 [12]	143.7M	92.36	95.13	96.10	0.9354	0.9237	0.9242	91.80	95.06	96.15	0.9296	0.9180	0.9187
MOBILENETV2 [53]	3.5M	92.38	94.98	96.05	0.9303	0.9238	0.9233	92.31	95.38	96.91	0.9311	0.9232	0.9225
WIDERESNET50_2 [54]	68.9M	92.46	96.28	97.28	0.9331	0.9247	0.9235	93.35	95.73	97.15	0.9421	0.9335	0.9330
RESNET50 [46]	25.6M	92.58	95.56	96.75	0.9332	0.9258	0.9252	93.08	96.48	97.20	0.9363	0.9308	0.9299
REGNETX32GF [55]	107.8M	92.86	95.71	96.93	0.9348	0.9287	0.9269	92.91	95.71	96.95	0.9366	0.9292	0.9282
DENSENET121 [56]	8.0M	92.93	95.75	96.88	0.9367	0.9293	0.9282	92.95	95.51	96.56	0.9360	0.9295	0.9285
RESNEXT101_32X8D [57]	88.8M	93.00	96.41	97.23	0.9364	0.9310	0.9303	94.20	96.61	97.58	0.9520	0.9420	0.9423
WIDERESNET101_2 [54]	126.9M	93.36	95.81	96.90	0.9423	0.9337	0.9332	92.73	96.35	97.63	0.9337	0.9273	0.9267
INCEPTIONV3 [58]	27.2M	93.50	96.48	97.35	0.9401	0.9350	0.9338	93.71	96.36	97.06	0.9446	0.9372	0.9371
DENSENET201 [56]	20.0M	93.56	95.78	96.73	0.9450	0.9357	0.9353	94.43	97.00	97.61	0.9492	0.9443	0.9442
RESNET101 [46]	44.5M	93.81	96.23	97.71	0.9432	0.9382	0.9406	93.23	96.93	98.13	0.9386	0.9323	0.9321
RESNET152 [46]	60.2M	94.06	97.06	98.05	0.9447	0.9407	0.9394	93.05	96.73	97.48	0.9374	0.9305	0.9297
RESNET34 [46]	21.8M	94.97	97.23	98.23	0.9516	0.9497	0.9491	91.98	95.95	97.20	0.9266	0.9198	0.9189
RESNET34 w/ Silhouette Polygonization	21.8M	92.72	96.41	97.51	0.9328	0.9272	0.9257	92.95 (+1.05%)	95.75	96.61	0.9352 (+0.93%)	0.9295 (+1.05%)	0.9283 (+1.02%)
RESNET34 w/ Topological Features	21.8M	93.72	96.43	97.78	0.9432	0.9372	0.9359	94.05 (+2.25%)	96.45 (+0.52%)	97.53 (+0.34%)	0.9476 (+2.27%)	0.9405 (+2.25%)	0.9401 (+2.31%)

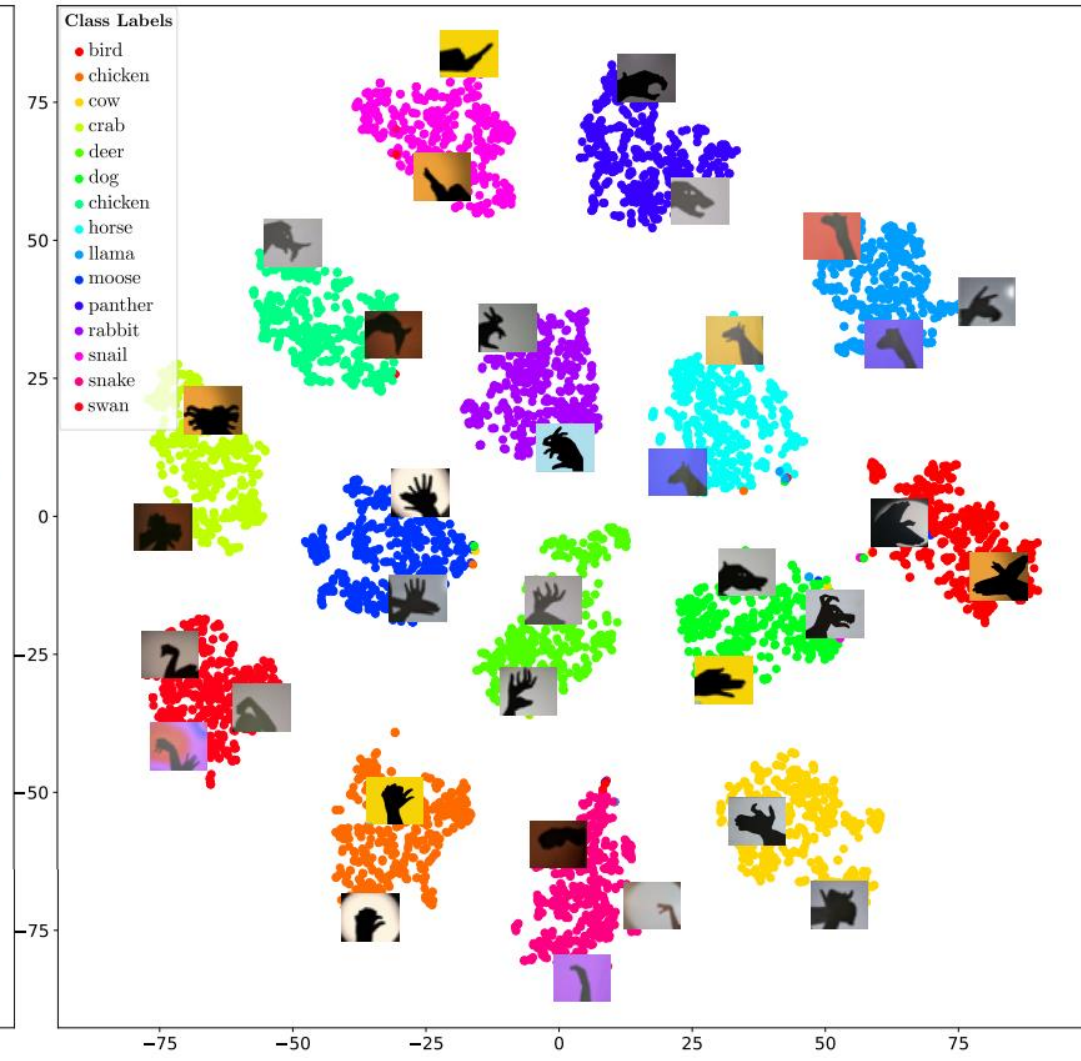
Results

Qualitative Analysis

Feature Space Visualization: t -SNE (t -Stochastic Neighbor Embedding)



(a) Vanilla ResNet34



(b) ResNet34 with Classifier Block

Results

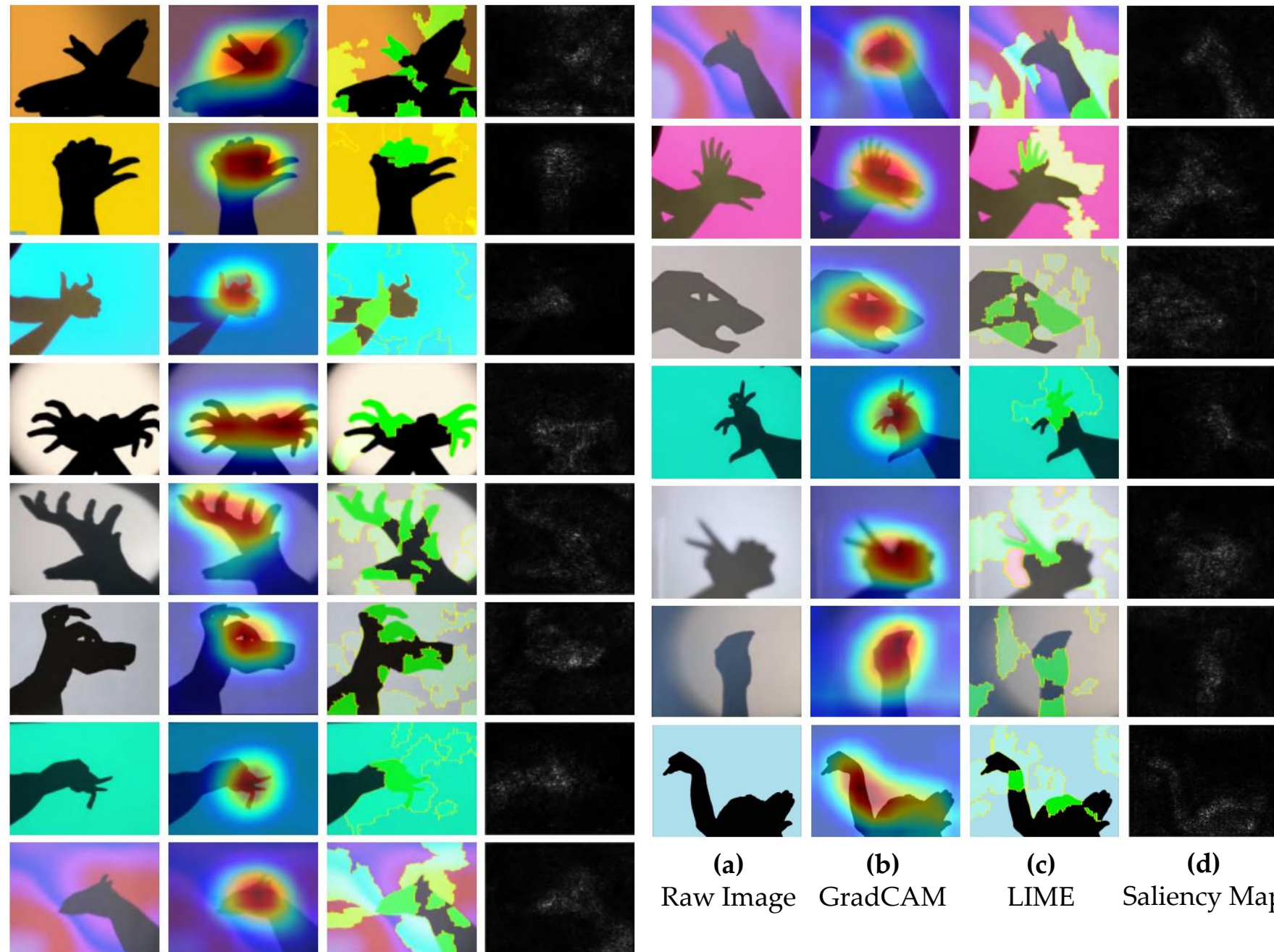
Qualitative Analysis

Explainable AI (xAI):

- GradCAM [12]
- LIME [13]
- Saliency Map [14]

Common-sense distinguishing features

- ✓ Bird wingspan, beak
- ✓ Chicken gallinaceous comb
- ✓ Cow horn, concave head
- ✓ Crab appendages
- ✓ Deer horns
- ✓ Dog slanted head, ears
- ✓ Elephant tusks, trunk
- ✓ Moose upright horns
- ✓ Panther eyes and ears
- ✓ Rabbit small hands and mouth
- ✓ Snail shell, antennae, etc.



Results

Error Analysis

Probable reasons for misclassifications:

- High Inter-Class Similarity
- Significant Intra-Class Variation
- Ambiguity of shape present in mid-action frames
- Poor lighting and ineptitude of the amateur child puppeteers

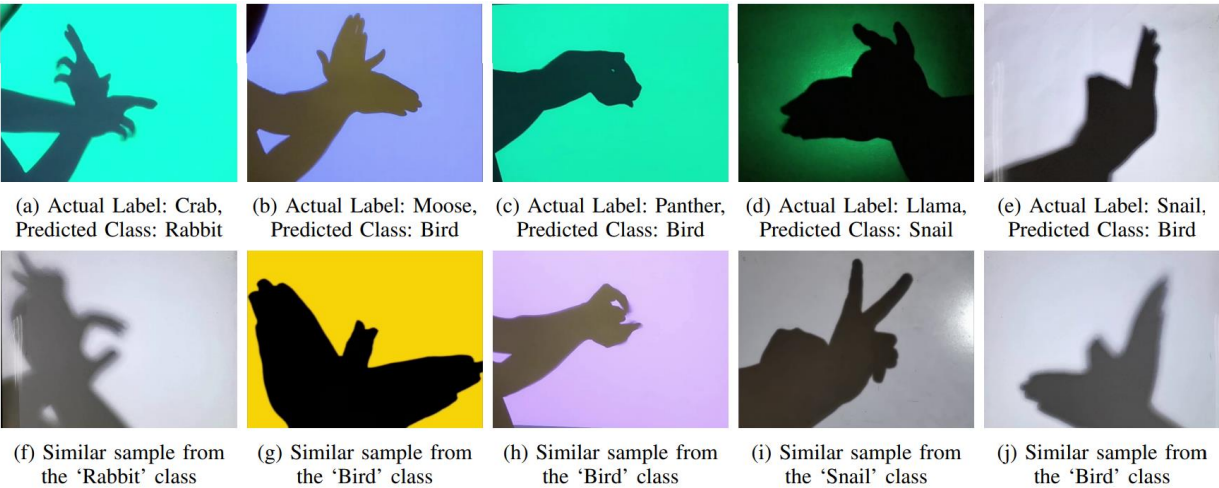


Fig: Misclassified samples with visually similar samples of the predicted class.

True Labels	Bird	Chicken	Cow	Crab	Deer	Dog	Elephant	Horse	Llama	Moose	Panther	Rabbit	Snail	Snake	Swan
	386	0	6	0	0	0	0	0	8	0	0	0	0	0	0
	2	396	1	0	0	0	0	0	0	0	0	0	0	1	0
	1	0	378	4	0	0	4	0	1	3	2	0	6	0	1
	18	1	1	323	0	2	0	0	2	23	0	30	0	0	0
	0	0	3	0	389	0	0	0	0	8	0	0	0	0	0
	2	0	0	0	0	391	0	1	4	0	0	0	2	0	0
	3	0	0	0	0	0	395	0	0	0	0	0	2	0	0
	0	0	1	0	0	4	0	395	0	0	0	0	0	0	0
	0	0	0	0	0	0	0	0	388	0	0	0	12	0	0
	6	1	0	4	2	0	0	0	0	387	0	0	0	0	0
	17	0	0	0	0	5	11	22	6	0	322	1	0	15	1
	1	1	0	4	0	0	1	0	0	0	0	390	2	0	1
	20	3	10	0	0	3	0	0	0	1	1	0	362	0	0
	0	0	0	0	0	0	0	0	0	0	0	0	0	399	1
	0	0	0	1	0	2	0	0	0	0	0	0	0	0	397
Predicted Labels															

Fig: Confusion Matrix of vanilla ResNet34.

Application: Digitization of Hand Shadow Puppetry

Mobile App Prototype

Objective: To create a real-time, interactive application that brings hand shadow puppetry to life using a lightweight trained model like MobileNetV2.

- Memory footprint: 29 MB
- Inference time: 880 μs

Snapdragon 8 Gen 2 of
Samsung Galaxy S23

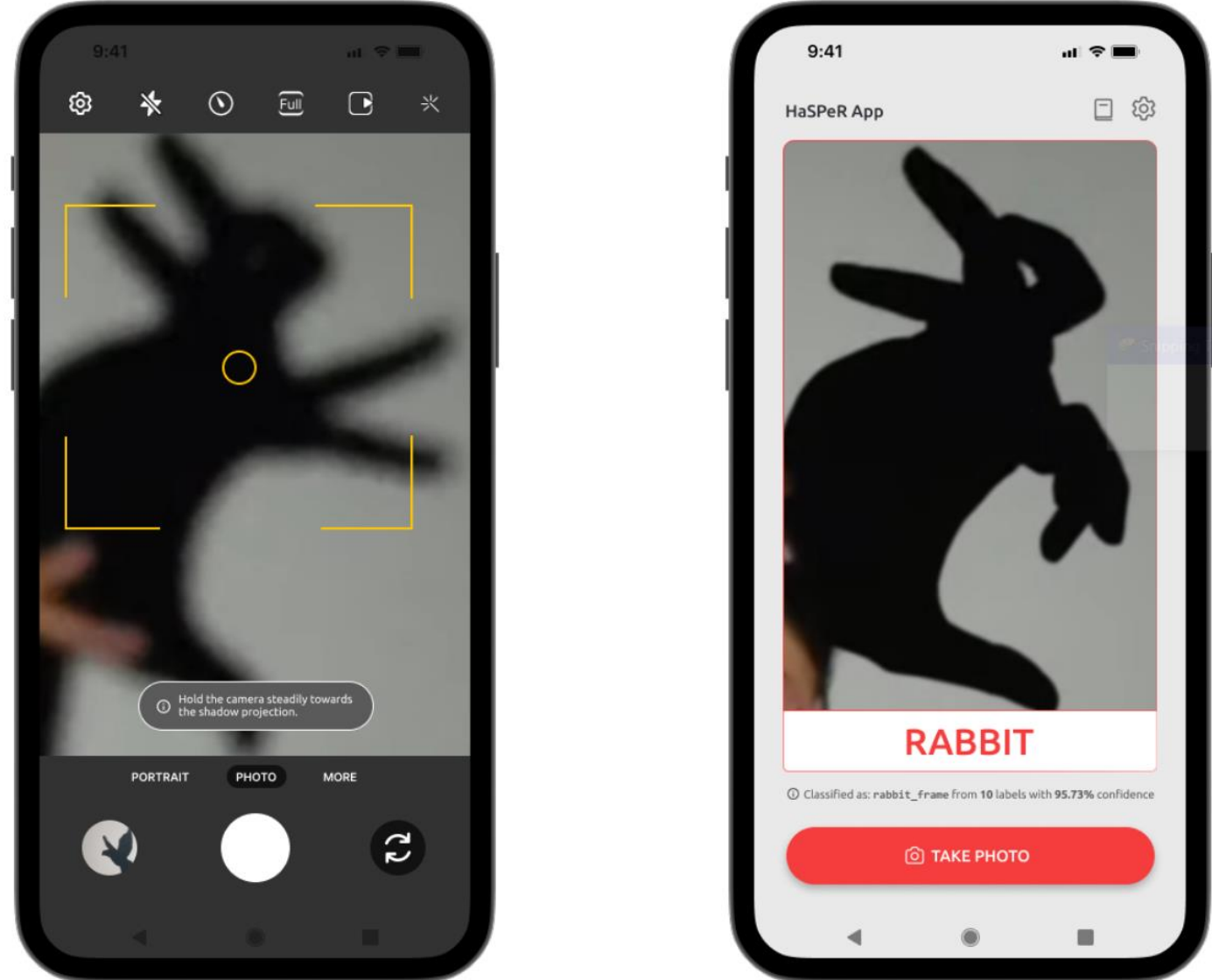
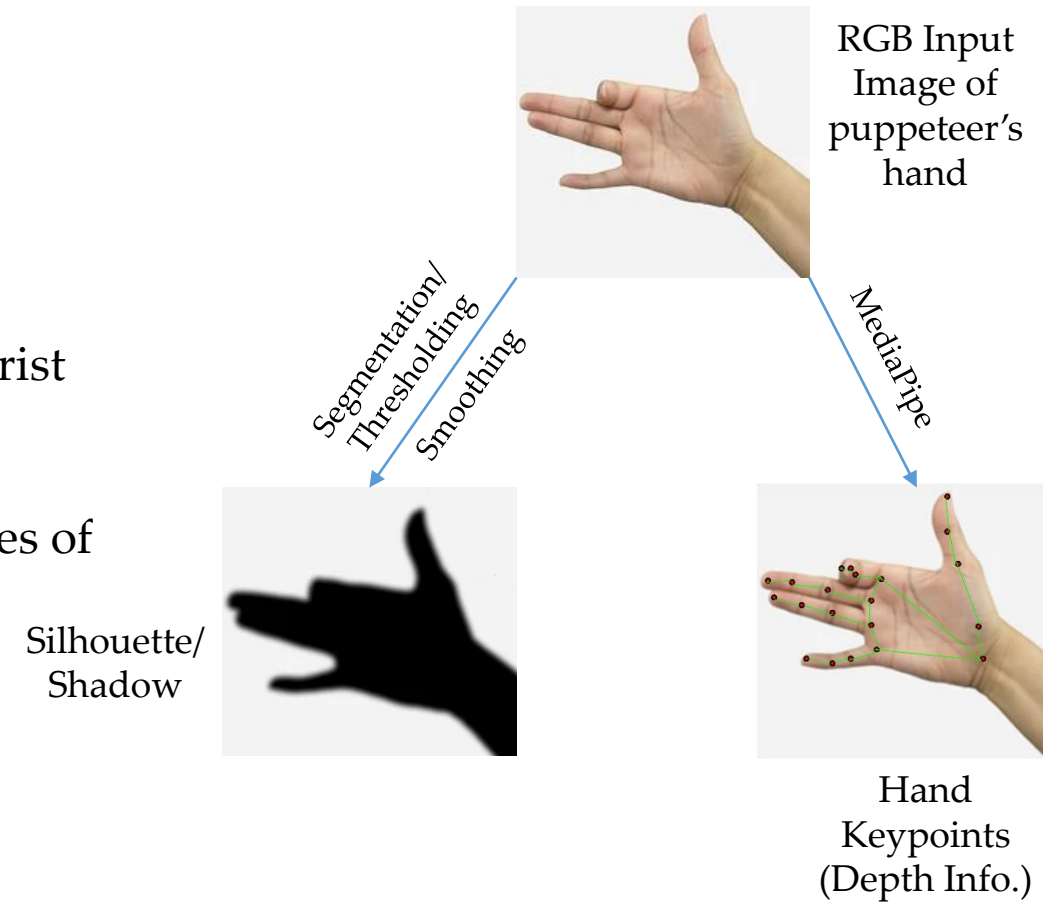


Fig: Android application for shadow puppet recognition.

Limitations

Scopes of Improvement

- Our work still has some ground to build upon:
 - ✓ Introducing samples with **more diversified** hand/palm/wrist structures.
 - ✓ Exploring **two different approaches** to classify RGB images of the hand
 - Feature Extraction after **RGB to grayscale silhouette conversion** (using pre-processing DIP techniques).
 - Utilizing **depth information** and coordinates of **hand landmarks** as features (using MediaPipe).
 - ✓ Yields **high accuracy in Sign Language Recognition** tasks, as per recently published research works.
 - ✓ Working on image/video generation.



Conclusion

Summary of our contributions

- We introduce **HASPER** (**H**and **S**hadow **P**uppet Image **R**epository), a novel, curated dataset of 15,000 images sourced from 68 professional and 90 amateur clips.
- We ensure diversity through variations in poses, orientations, background lighting, and silhouette motion via **optical flow estimation**.
- We evaluate **31 state-of-the-art pretrained image classification models** on HASPER to establish integrity baselines.
- We thoroughly assess **ResNet34**'s feature representations, feature fusions, interpretability, explainability, and classification errors.
- We develop a **lightweight Android app** using Flutter for real-time classification of hand shadow puppets from camera feeds, showcasing potential for digitized ombromanie learning tools.
- Our core finding is: **Skip-connected Convolutional models > Attention-based Transformers models**.
(skip-connections help **preserve** low-level edge and contour information through **identity mappings**)

References

Works cited in this presentation

- [1] A. Almoznino and Y. Pinas, “The art of hand shadows,” pp. 1–64, 2002.
- [2] F. Lu, F. Tian, Y. Jiang, X. Cao, W. Luo, G. Li, X. Zhang, G. Dai, and H. Wang, “Shadowstory: creative and collaborative digital storytelling inspired by cultural heritage,” in *Proceedings of the SIGCHI Conference on Human Factors in Computing Systems*, ser. CHI '11. Vancouver BC, Canada: ACM, May 2011, p. 1919–1928.
- [3] Z. Huang, V. K. Madaram, S. Albadrani, and T. V. Nguyen, “Shadow puppetry with robotic arms,” in *Proceedings of the 25th ACM international conference on Multimedia*, pp. 1251–1252, 2017.
- [4] H. Zhang, Y. Song, Z. Chen, J. Cai, and K. Lu, “Chinese shadow puppetry with an interactive interface using the kinect sensor,” in *Computer Vision–ECCV 2012. Workshops and Demonstrations: Florence, Italy, October 7–13, 2012, Proceedings, Part I 12*, pp. 352–361, Springer, 2012.
- [5] B. M. Carr and G. J. Brown, “Shadow puppetry using the kinect,” 2014.
- [6] M. Huang, S. Mehrotra, and F. Sparacino, “Shadow vision,” 1999.
- [7] <https://www.kaggle.com/datasets/deepshah16/silhouettes-of-human-posture>
- [8] B. D. Lucas and T. Kanade, “An iterative image registration technique with an application to stereo vision,” in *Proceedings of the 7th International Joint Conference on Artificial Intelligence*, vol. 2. San Francisco, CA, USA: Morgan Kaufmann Publishers Inc., 1981, pp. 674–679.
- [9] C. Zach, T. Pock, and H. Bischof, A Duality Based Approach for Realtime TV-L 1 Optical Flow. *Springer Berlin Heidelberg*, p. 214–223. [Online]. Available: http://dx.doi.org/10.1007/978-3-540-74936-3_22

References

Works cited in this presentation

- [10] D. H. Douglas and T. K. Peucker, "Algorithms for the reduction of the number of points required to represent a digitized line or its caricature," *Cartographica: The International Journal for Geographic Information and Geovisualization*, vol. 10, no. 2, pp. 112–122, 1973. [Online]. Available: <https://doi.org/10.3138/FM57-6770-U75U-7727>
- [11] H. Blum, "A Transformation for Extracting New Descriptors of Shape," in *Models for the Perception of Speech and Visual Form*, W. Wathen-Dunn, Ed. Cambridge, MA: The MIT Press, 1967, pp. 362–380.
- [12] R. R. Selvaraju, M. Cogswell, A. Das, R. Vedantam, D. Parikh, and D. Batra, "Grad-cam: Visual explanations from deep networks via gradient-based localization," in *2017 IEEE International Conference on Computer Vision (ICCV)*. Venice, Italy: IEEE, Oct. 2017, p. 618–626.
- [13] M. Ribeiro, S. Singh, and C. Guestrin, "'why should I trust you?': Explaining the predictions of any classifier," in *Proceedings of the 2016 Conference of the North American Chapter of the Association for Computational Linguistics: Demonstrations*, J. DeNero, M. Finlayson, and S. Reddy, Eds. San Diego, California: Association for Computational Linguistics, Jun. 2016, pp. 97–101.
- [14] K. Simonyan, A. Vedaldi, and A. Zisserman, "Deep inside convolutional networks: visualising image classification models and saliency maps," in *Proceedings of the ICLR*, 2014.

THANK YOU FOR LISTENING.

GET IN TOUCH:

EMAIL — {rifatraiyan, zibranzarif, sabbirahmed}@iut-dhaka.edu

TWITTER — @realRifatRaiyan

